

BRAF Inhibition Increases Tumor Infiltration by T cells and Enhances the Antitumor Activity of Adoptive Immunotherapy in Mice

Chengwen Liu¹, Weiyi Peng¹, Chunyu Xu¹, Yanyan Lou¹, Minying Zhang¹, Jennifer A. Wargo⁴, Jie Qing Chen¹, Haiyan S. Li², Stephanie S. Watowich², Yan Yang¹, Dennie Tompers Frederick⁴, Zachary A. Cooper⁴, Rina M. Mbofung¹, Mayra Whittington¹, Keith T. Flaherty⁵, Scott E. Woodman¹, Michael A. Davies^{1,3}, Laszlo G. Radvanyi¹, Willem W. Overwijk¹, Gregory Lizée¹, and Patrick Hwu¹

Abstract

Purpose: Treatment of melanoma patients with selective BRAF inhibitors results in objective clinical responses in the majority of patients with *BRAF*-mutant tumors. However, resistance to these inhibitors develops within a few months. In this study, we test the hypothesis that BRAF inhibition in combination with adoptive T-cell transfer (ACT) will be more effective at inducing long-term clinical regressions of *BRAF*-mutant tumors.

Experimental Design: *BRAF*-mutated human melanoma tumor cell lines transduced to express gp100 and H-2D^b to allow recognition by gp100-specific pmel-1 T cells were used as xenograft models to assess melanocyte differentiation antigen-independent enhancement of immune responses by BRAF inhibitor PLX4720. Luciferase-expressing pmel-1 T cells were generated to monitor T-cell migration *in vivo*. The expression of VEGF was determined by ELISA, protein array, and immunohistochemistry. Importantly, VEGF expression after BRAF inhibition was tested in a set of patient samples.

Results: We found that administration of PLX4720 significantly increased tumor infiltration of adoptively transferred T cells *in vivo* and enhanced the antitumor activity of ACT. This increased T-cell infiltration was primarily mediated by the ability of PLX4720 to inhibit melanoma tumor cell production of VEGF by reducing the binding of c-myc to the VEGF promoter. Furthermore, analysis of human melanoma patient tumor biopsies before and during BRAF inhibitor treatment showed downregulation of VEGF consistent with the preclinical murine model.

Conclusion: These findings provide a strong rationale to evaluate the potential clinical application of combining BRAF inhibition with T-cell-based immunotherapy for the treatment of patients with melanoma. *Clin Cancer Res*; 19(2); 393–403. ©2012 AACR.

Introduction

The identification of activating point mutations of the *BRAF* gene, present in approximately half of all human cutaneous melanomas, has proven to be a milestone for

contributing not only to our understanding of melanoma biology but also for changing the treatment and clinical outcomes of the disease (1). As a component of the RAS-RAF-MEK-MAPK signal transduction pathway, *BRAF* is also mutated to a constitutively activated form in many other cancers, including thyroid, colorectal, and hairy cell leukemia (1–6). Although more than 50 distinct mutations in *BRAF* have been described to date, a valine to glutamic acid substitution at amino acid position 600 (V600E), is by far the most frequent, comprising more than 70% of *BRAF* mutations in melanoma (1, 7). Thus, *BRAF*(V600E) being so widely expressed, has provided a strong rationale for the development and clinical application of small-molecule-based pharmaceutical inhibitors that selectively target *BRAF*(V600E) to treat patients with metastatic melanoma, whose treatment options are limited (8–11).

Recent clinical trials have shown that over half of melanoma patients with *BRAF*(V600E)-expressing tumors experience objective clinical responses to selective inhibitors of *BRAF*. However, complete and durable remissions

Authors' Affiliations: Departments of ¹Melanoma Medical Oncology and ²Immunology, Center for Cancer Immunology Research; ³Department of Systems Biology, Division of Cancer Medicine, The University of Texas MD Anderson Cancer Center, Houston, Texas; Divisions of ⁴Surgical Oncology and ⁵Medical Oncology, Massachusetts General Hospital, Boston, Massachusetts

Note: Supplementary data for this article are available at Clinical Cancer Research Online (<http://clincancerres.aacrjournals.org/>).

C. Liu and W. Peng contributed equally to this work.

Corresponding Author: Patrick Hwu, Department of Melanoma Medical Oncology, The University of Texas MD Anderson Cancer Center, 1515 Holcombe Blvd, Houston, TX 77030. Phone: 713-563-1728; Fax: 713-745-1046; E-mail: phwu@mdanderson.org

doi: 10.1158/1078-0432.CCR-12-1626

©2012 American Association for Cancer Research.

Translational Relevance

BRAF-targeted therapy has resulted in objective responses in the majority of patients with melanoma harboring the BRAF(V600E) mutation; however, the median duration of response is less than a year. There is evidence for immune evasion in BRAF-mutant melanoma, which may be reversed with BRAF-targeted therapy, strongly implicating the rationale for a BRAF-targeted therapy in combination with immunotherapy. Adoptive T-cell transfer (ACT) therapy using tumor-infiltrating lymphocytes is one of the most promising immunotherapeutic approaches for melanoma treatment resulting in objective responses for more than 50% of treated patients. Here, we report that BRAF inhibition in melanoma increases the T-cell infiltration into tumors, via decreased VEGF production, and enhances the antitumor activity of ACT therapy. Our findings provide a rationale of combining BRAF inhibitor with ACT therapy for clinical application to improve durable response rates to therapy.

were rarely observed in these patients, and disease relapses accompanied by BRAF inhibitor resistance typically occurred within a year (12, 13). The mechanisms that cause resistance are diverse and include mitogen-activated protein kinase (MAPK) pathway reactivation by alternate means (14–19). Hence, to improve long-term clinical responses and avoid selection of drug-resistant tumors, combination therapies that target multiple pathways have been proposed (3, 4, 20).

Although therapeutic approaches that combine small-molecule-based inhibition of multiple signal transduction pathways has been an area of ongoing investigation, 1 alternative involves the combination of BRAF inhibitors with immune-based therapies. This approach seems particularly promising due to the emerging link between MAPK pathway activation in cancer and the suppression of anti-tumor immunity. For example, knockdown of BRAF (V600E) in melanoma cell lines has been shown to decrease the production of immunosuppressive soluble factors, such as interleukin (IL)-10, VEGF, and IL-6 (21). Recent *in vitro* experiments showed that blocking of MAPK signaling in melanoma cells could increase the expression of melanocyte differentiation antigens (MDA), leading to improved recognition by MDA-specific T cells (22, 23). In addition, a study by Jiang and colleagues showed that the paradoxical activation of MAPK promoted programmed death ligand 1 (PD-L1) expression in melanoma cells resistant to BRAF inhibition (24). Perhaps most importantly, the exquisite specificity of recently developed small-molecule inhibitors that target mutated oncogenes have shown little or no detrimental effects on immune cells that also use the MAPK pathway (23, 25).

In the current preclinical study, we assessed whether the addition of a selective BRAF(V600E) inhibitor could

improve the efficacy of T cell-based immunotherapy *in vivo*. We found that adoptive T-cell transfer (ACT) with melanoma-specific T cells was much more effective in the context of concurrent BRAF inhibition, which led to increased T-cell infiltration of tumors that could be attributed largely to decreased VEGF production by the tumor cells. Furthermore, a subset of responding patients with melanoma showed similar changes in the tumor microenvironment following BRAF-inhibitor treatment, providing a strong rationale to explore the use of combination treatments involving MAPK pathway inhibition and T cell-based immunotherapy.

Materials and Methods

Animals and cell lines

C57BL/6, C57BL/6J-Tyr-2/J albino, and pmel-1 TCR transgenic mice on a C57BL/6 background were purchased from the Jackson Laboratory. B6 nude mice were purchased from the Taconic Farms. All mice were maintained in a specific pathogen-free barrier facility at The University of Texas MD Anderson Cancer Center (Houston, TX). Mice were handled in accordance with protocols approved by the Institutional Animal Care and Use Committee. A375 (BRAF V600E⁺), Mel624 (BRAF V600E⁺/HLA-A2⁺/MART-1⁺), WM35 (BRAF V600E⁺/HLA-A2⁺/gp100⁺/MART-1⁺), MEWO (BRAF Wild-Type/HLA-A2⁺/MART-1⁺), and C918 (BRAF Wild-Type) human melanoma cell lines and MC38 murine colon adenocarcinoma cell line were maintained in RPMI-1640 medium supplemented with 10% heat-inactivated FBS, and penicillin-streptomycin (all from Invitrogen). MART-1-reactive DMF5 T cells were obtained from the National Cancer Institute (26) and cultured in RPMI-1640 medium containing 10% heat-inactivated human AB serum (Valley Biomedical), β -Mercaptoethanol (Invitrogen) and recombinant human IL-2 (TECIN, National Cancer Institute Biological Resources Branch).

Patient samples

Patients with metastatic melanoma possessing BRAF (V600E) mutation were enrolled on clinical trials for treatment with a BRAF inhibitor (RO5185426) or combined BRAF + MEK inhibitor (GSK2118436 + GSK1123212) and were consented for tissue acquisition per Institutional Review Board (IRB)-approved protocol. Tumor biopsies were conducted pretreatment (day 0), at 10 to 14 days on treatment.

Generation of luciferase-expressing pmel-1 T cells

Splenocytes from pmel-1 mice were cultured in complete medium containing 300 IU/mL IL-2, and 0.3 μ g/mL anti-mouse CD3 (BD Bioscience). After 24 hours, the cells were infected with a retroviral vector encoding a modified firefly luciferase gene *OFL* and *GFP*, as previously described (27, 28). Three days after viral transduction, cells were sorted by a FACSAria (BD Bioscience) based on expression of GFP.

Bone marrow–derived dendritic cells

Dendritic cells were generated from murine bone marrow cells as previously described (29, 30). Dendritic cells pulsed with 10 $\mu\text{mol/L}$ H-2D^b-restricted gp100 peptide (KVPRNQDWL) for 3 hours at 37°C on day 7. After wash with PBS, dendritic cells were immediately injected into mice.

Lentiviral transduction of tumor cells

Lentiviral vectors and packaging vectors, VSV-G and $\Delta 8.9$, were cotransfected into 293T cells using Lipofectamine 2000, and supernatant was collected after 36 hours culture. A total of 1×10^6 tumor cells were preseeded in each well of 6-well plates for 6 hours and spun at $850 \times g$ for 1 hour with 1 mL virus supernatant and 8 $\mu\text{g/mL}$ polybrene. The following day, the supernatant was removed and replaced with growth medium. Infected tumor cells were collected and sorted on the basis of the expression of the reporter gene using a FACSAria.

Adoptive transfer, vaccination, and treatment

B6 nude mice were subcutaneously implanted with 6 to 10×10^6 melanoma cells on day 0. When tumors were established, 1×10^6 luciferase-transduced pmel-1 T cells were adoptively transferred into tumor-bearing mice, followed by intravenous injection of 0.5×10^6 peptide-pulsed dendritic cells. IL-2 (5×10^5 IU/mouse) was intraperitoneally administered twice daily for 3 days after T-cell transfer. Two days after T-cell transfer, PLX4720 (provided by Plexxikon) was administered for 3 days. PLX4720 powder was suspended in vehicle [3% dimethyl sulfoxide (DMSO), 1% methylcellulose] and administered by oral gavage daily (100 mg/kg). In some experiments, mice were fed by a chow diet containing 417 mg/kg PLX4720. For anti-VEGF treatment, anti-hVEGF antibody (Ab; hybridoma, A4.6.1 from American Type Culture Collection) was administered at 250 $\mu\text{g}/\text{mouse}$ on day 7, 9, and 11. Mouse immunoglobulin G (IgG) was used as control Ab. Because antitumor response of ACT is dependent on lymphodepletion (31), in some experiments using C57BL/6J-Tyr-2/J albino mice as recipients, lymphopenia was induced by administering a nonmyeloablative dose (350 cGy) of radiation 1 day before adoptive transfer. Tumor sizes were monitored by measuring the perpendicular diameters of the tumors. All experiments were carried out in a blinded, randomized fashion.

In vivo bioluminescence imaging

Mice were intraperitoneally injected with 100 μL of 20 mg/mL D-luciferin (Xenogen). Eight minutes later, mice anesthetized with isoflurane were imaged using an IVIS 200 system (Xenogen), according to the manufacturer's manual. Living Image software (Xenogen) was used to analyze data. Regions of interest (ROI) were manually selected and quantification is reported as the average of photon flux within ROI. The bioluminescence signal is represented as photons/s/cm²/sr.

IFN- γ secretion assay

Melanoma cells were pretreated with various concentrations of PLX4720 for 48 hours, then were washed 3 times with culture medium. After counting, tumor cells were cocultured with DMF5 or pmel-1 T cells at 5×10^4 per well (1:1 ratio) as triplicates for 24 hours, with or without adding back PLX4720. IFN- γ production was determined in culture supernatants using an ELISA kit (BioLegend).

Cytotoxicity assay

Melanoma cells were pretreated with PLX4720 or vehicle (DMSO) for 48 hours. After washing and counting, melanoma cells were labeled with ⁵¹Cr, and then cocultured with activated pmel-1 T cells at different effector-to-target (E:T) ratios. Four hours later, ⁵¹Cr release was determined against target cells. Specific ⁵¹Cr release was calculated using the standard formula: [(sample release – spontaneous release)/(total release – spontaneous release)] \times 100%.

hVEGF secretion assay

Melanoma cells were treated with various concentrations of PLX4720 for 24 hours, with DMSO added as a vehicle control. The supernatants were then harvested for ELISA assay (R&D System), and the cells were harvested and counted.

Proliferation assay

DMF5 cells (5×10^4 /well) were cultured with IL-2 (300 IU/mL) at various concentrations with PLX4720 in an OKT3 precoated (1 $\mu\text{g}/\text{mL}$, 100 $\mu\text{L}/\text{well}$, 4°C for overnight) 96-well plate for 56 hours. [³H]Thymidine (5 $\mu\text{Ci}/\text{mL}$) was then added for a further 16 hours, and [³H]Thymidine incorporation was quantified in a liquid scintillation counter.

Cell viability assay

Melanoma cells were seeded in flat-bottom 96-well plates and treated with various concentration of PLX4720 for 72 hours, with DMSO added as a vehicle control. Cell viability was determined using CellTiter-Blue Cell Viability assay (Promega).

Protein arrays

A375 tumor-bearing mice were sacrificed 3 days after oral gavage of PLX4720, and tumors were resected and weighed. Tumors were homogenized and sonicated in lysis buffer containing protease inhibitors. Cleared tumor lysates after centrifugation were tested using the Searchlight protein array, according to the manufacturer's protocol (Aushon Biosystems).

ChIP arrays

A375 cells were treated with PLX4720 (1 $\mu\text{mol/L}$) or DMSO for 2 hours, followed by a chromatin immunoprecipitation (ChIP) assay, conducted according to the manufacturer's instructions (Millipore). Briefly, the protein–DNA complexes were cross-linked and immunoprecipitated with anti-c-myc, anti-p300, and anti-E2F1 antibodies or rabbit

control IgG. After reversing the cross-linking, real-time PCR was used to amplify sequences corresponding to the promoter regions of human VEGF or control gene *GAPDH*.

Flow-cytometric analysis

Peripheral blood or tumors were harvested at the indicated time points. Tumor tissues were weighed and dissociated. After depletion of erythrocytes using ammonium-chloride-potassium lysing buffer (Invitrogen), the remaining lymphocytes were treated with Fc blocking monoclonal antibodies (mAbs; anti-CD16/32 2.4G2) and then stained with mAbs against Thy1.1 and CD45 (BD Biosciences). Samples were analyzed using a FACSCalibur or FACSCanto II (BD Biosciences).

Immunohistochemistry

Immunohistochemical staining was carried out using the Avidin–Biotin Complex Kit (Vector Laboratories). Nine tumor samples of patient with melanoma before and following treatment with BRAF inhibitor were stained for VEGF (1:100, Abcam) and mouse xenograft tumor samples were stained for CD3 (1:100, Abcam). Samples were appropriately optimized in our laboratory, and external controls were systemically used to avoid false-negative or false-positive staining. Percentages of VEGF-stained tumor cells were quantitated using microscopy and pathologic examination. CD3⁺ T cell counts were conducted on slides in 10 adjacent high-power fields (HPF, ×400) based on lymphocyte morphology.

Quantitative PCR

Differential expression of VEGF in patient samples was assayed using TaqMan Gene Expression Assays (Applied

Biosystems) with actin as control. mRNA was reverse transcribed to cDNA using SuperScript VILO (Invitrogen)

Statistical analysis

Comparisons of differences in continuous variables between 2 groups were done using Student *t* test. Differences in tumor size and T-cell numbers among different treatments were evaluated by ANOVA repeated-measures function. The statistical analysis to compare survival was determined using Kaplan–Meier test. *P* values are based on 2-tailed tests, with *P* < 0.05 considered statistically significant.

Results

A human melanoma xenograft model to assess MDA-independent enhancement of immune responses by PLX4720

To investigate the effects of BRAF inhibition on tumor cell recognition by T cells, 3 HLA-A2⁺ melanoma cell lines were pretreated for 48 hours with titrated doses of the selective BRAF inhibitor PLX4720, and then cocultured with HLA-A2–restricted MART-1–specific T cells. T-cell recognition, as measured by IFN- γ secretion, increased in a dose-dependent fashion in the 2 melanoma cell lines expressing BRAF (V600E) but not in the cell line expressing wild-type (WT) BRAF (Supplementary Fig. S1A–S1C). These results imply that PLX4720 can enhance MART-1–specific T-cell recognition of melanoma cells, consistent with the findings of a previous study showing upregulation of MDA by PLX4720 (23). Furthermore, when PLX4720 was added to the culture system, neither T-cell cytokine secretion function nor TCR mAb-induced proliferation was inhibited at concentrations as high as 1 μ mol/L (Supplementary Fig. S1A–S1D). Thus,

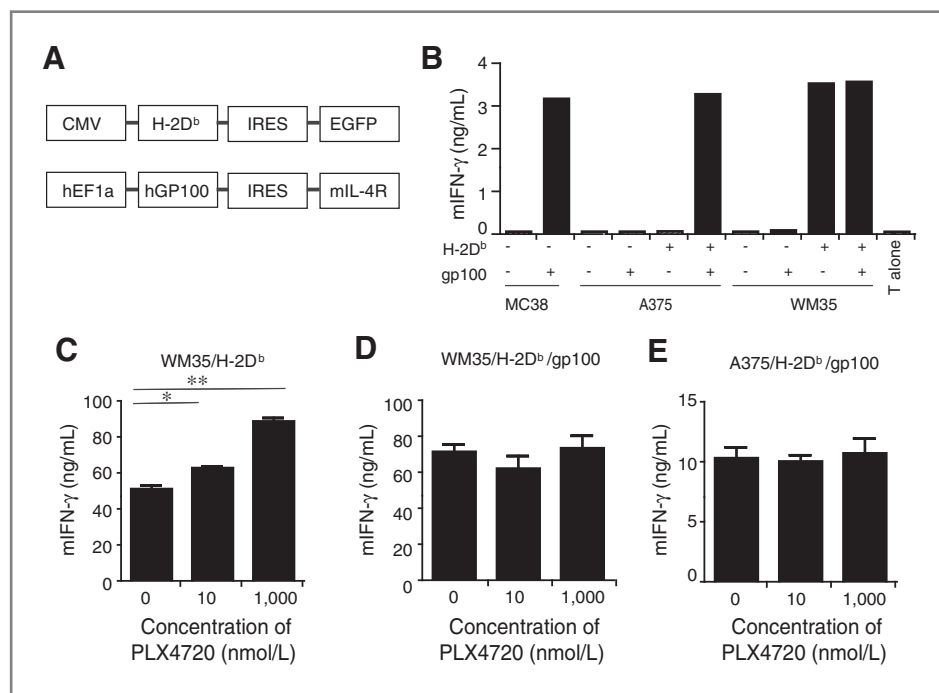


Figure 1. Overexpression of gp100 abrogates enhanced melanoma T-cell recognition induced by PLX4720. A, schematic representation of 2 lentiviral vectors containing full-length human gp100 and mL-4R, or H-2D^b and EGFP. B, IFN- γ secretion by pmel-1 T cells cocultured with the indicated transduced tumor cell lines (before cell sorting) for 24 hours, as determined by ELISA. Untransduced MC38 murine colon adenocarcinoma cells or those transduced with gp100 were used as negative and positive controls, respectively. C–E, IFN- γ secretion by pmel-1 T cells cocultured with transduced melanoma cells (after cell sorting) that had been pretreated with the indicated concentrations of PLX4720, as determined by ELISA (*, *P* < 0.05; **, *P* < 0.01). Data are representative of 3 independent experiments. IRES, internal ribosome entry site.

selective BRAF(V600E) inhibition does not significantly inhibit T-cell proliferation, similar to results we have previously reported that analyzed circulating immune cells from patients with melanoma before and following treatment with a selective BRAF inhibitor (25).

Although upregulation of MDA is one mechanism by which BRAF inhibition can enhance immune recognition of melanoma, we hypothesized that this class of antigen represents only a small fraction of melanoma-reactive T cells in the tumor microenvironment, and that BRAF inhibition could be having other more global influences on the immune response. To study these potential alternative mechanisms, we engineered the human BRAF(V600E)-positive melanoma cell line A375 to constitutively express high levels of the gp100 melanoma tumor antigen under control of the cytomegalovirus (CMV) promoter, thus eliminating any influence of the BRAF inhibitor on the expression of this MDA. The A375 cell line was also engineered to express murine H-2D^b (Fig. 1A) to enable recognition by murine gp100-specific transgenic pmel-1 T cells.

To test the validity of this approach, a series of *in vitro* experiments were carried out to confirm that gp100 overexpression did, in fact abrogate enhanced T-cell reactivity induced by PLX4720. As shown in Fig. 1B, pmel-1 cells could only recognize and secrete IFN- γ in response to A375 cells transduced to express both H-2D^b and gp100 (A375/H-2D^b/gp100). In contrast, human WM35 melanoma cells that naturally express gp100 were recognized when transduced with only H-2D^b. As a further control, the murine

colorectal carcinoma cell line MC38 that naturally expresses H-2D^b could only be recognized by pmel-1 T cells upon transduction with gp100. As shown in Fig. 1C and D, PLX4720 treatment could enhance pmel-1 T-cell recognition of WM35 cells transduced with H-2D^b but not when these cells were also transduced to overexpress gp100. Similarly, PLX4720 treatment of A375 cells transduced to express both H-2D^b and gp100 did not induce enhanced pmel-1 T-cell recognition, as measured by IFN- γ secretion or cytotoxicity (Fig. 1E and Supplementary Fig. S2). Therefore, this xenogeneic tumor model was determined to be appropriate for evaluating the effects on immune responses *in vivo* by PLX4720 that were independent of its impact on MDA expression.

BRAF inhibition increases tumor infiltration of adoptively transferred T cells and enhances antitumor responses

We next sought to investigate whether PLX4720 could enhance the efficacy of ACT *in vivo*. B6 nude mice were subcutaneously implanted with A375/H-2D^b/gp100 melanoma cells and then treated with a combination of OFL-expressing pmel-1 T cells and peptide-pulsed dendritic cells as previously described (30) followed by PLX4720 administration. Tumor sizes and T-cell migration were monitored over time. As shown in Fig. 2A and B, administration of PLX4720 led to approximately 10-fold higher luciferase intensity at the tumor site, compared with vehicle control. The increased T-cell infiltration was confirmed by

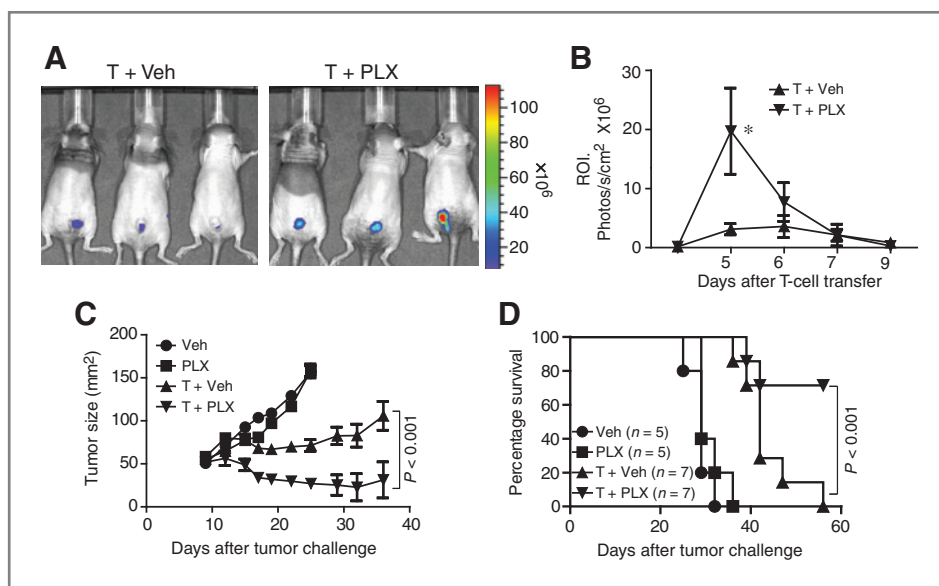


Figure 2. Administration of PLX4720 *in vivo* increases tumor infiltration of adoptively transferred T cells and enhances antitumor responses. A, B6 nude mice (5 mice/group) bearing A375/H-2D^b/gp100 tumors were treated with OFL-expressing pmel-1 T cells, along with gp100 peptide-pulsed dendritic cells, by intravenous injection on day 7 after tumor inoculation. Two days after T-cell transfer, PLX4720 or vehicle alone was administered by oral gavage daily for 3 days. Luciferase imaging showing *in vivo* trafficking of OFL-expressing pmel-1 T cells on day 5 after T-cell transfer. B, summary of quantitative imaging analysis of transferred T cells at the tumor site. Quantification is expressed as the average of photon flux within ROI (*, $P < 0.05$). C, B6 nude mice (5–7 mice/group) bearing A375/H-2D^b/gp100 tumors were treated with pmel-1 T cells and gp100 peptide-pulsed dendritic cells, by intravenous injection on day 10 after tumor inoculation. Two days after T-cell transfer, mice were fed a diet containing PLX4720 or vehicle for 3 days, and tumor growth was monitored over time. D, mouse survival as monitored over time following treatment. Data shown are expressed as mean \pm SEM and are representative of 2 to 3 independent experiments with similar results.

immunohistochemical staining for CD3 and flow cytometry for Thy1.1+ pmel-1 T cells (Supplementary Fig. S3A–S3D). This higher level of tumor antigen-specific pmel-1 T-cell infiltration was associated with antitumor responses that were significantly better than those observed in mice treated with either PLX4720 or ACT alone (Fig. 2C). As shown in Fig. 2D, extended survival was also observed in the combination therapy group. The percentage of pmel-1 T cells in peripheral blood did not differ between the treatment groups (Supplementary Fig. S4), suggesting that administration of PLX4720 can enhance the antitumor activity of ACT through increasing T-cell migration to tumor sites.

To understand if expression of tumor antigen is necessary for T-cell accumulation in tumors treated with PLX4720, B6 nude mice were subcutaneously implanted with non-gp100-expressing A375/H-2D^b melanoma cells and then treated with ACT in combination with PLX4720 or vehicle control. As shown in Supplementary Fig. S5A and S5B, PLX4720 treatment cannot significantly increase T-cell infiltration in A375/H-2D^b tumors. These results suggest that tumor antigen expression is important for PLX4720-induced T-cell infiltration into tumors.

PLX4720 increases infiltration of adoptively transferred T cells only in tumors with a BRAF(V600E) mutation

The impact of RAF inhibitors on inhibiting extracellular signal-regulated kinase (ERK) signaling in tumor cells with

mutant *BRAF* has been extensively investigated (9, 20), but recent studies have also shown that BRAF inhibitors can enhance ERK signaling in cells with wild-type *BRAF* (32–34). To exclude the possibility that PLX4720 increased intratumoral T-cell accumulation via directly acting on the transferred T cells, we repeated the *in vivo* tumor treatment experiments using tumors with and without the BRAF (V600E) mutation. As expected, PLX4720 was not capable of inhibiting the *in vitro* growth of C918 melanoma cells, which have a wild-type *BRAF* (Fig. 3A). However, transduction with H-2D^b and gp100 did render C918 cells susceptible to recognition by pmel-1 T cells (Fig. 3B). Comparing antitumor responses against C918 and A375 *in vivo*, we found that addition of PLX4720 to the ACT regimen led to an increase in luciferase intensity in A375/H-2D^b/gp100 but not in C918/H-2D^b/gp100 tumors (Fig. 3C and D). This result suggested that PLX4720 could only enhance infiltration of adoptively transferred T cells in tumors containing a BRAF(V600E) mutation, a finding that was confirmed using another BRAF(V600E) cell line WM35/H-2D^b/gp100 (Supplementary Fig. S6A–S6C) and another wild-type *BRAF* cell line, MC38/gp100 (Supplementary Fig. S7A–S7C).

PLX4720 increases infiltration of adoptively transferred T cells by inhibiting the production of VEGF in tumors

Because PLX4720 augmented the infiltration of T cells into *BRAF* mutant but not wild-type tumors, we next explored potential differences in the tumor

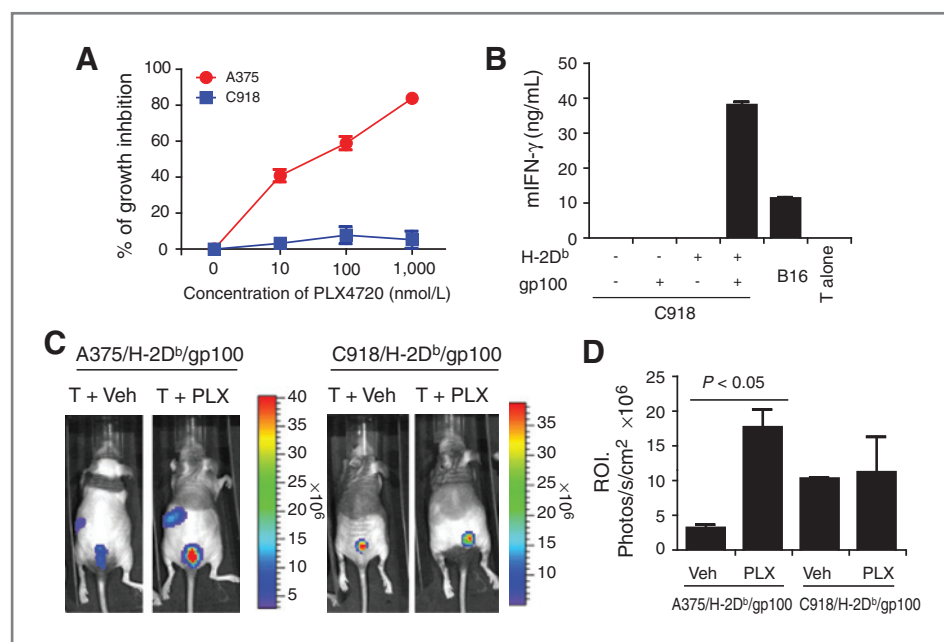


Figure 3. PLX4720 increases infiltration of adoptively transferred T cells only in tumors containing BRAF(V600E). A, growth inhibition of BRAF(V600E)-mutated (A375) and WT (C918) human melanoma cell lines treated *in vitro* with PLX4720 for 72 hours, as determined by a CellTiter-Blue Cell Viability assay. B, IFN- γ secretion by pmel-1 T cells cocultured with C918 melanoma cells expressing gp100 and/or H-2D^b for 24 hours, as determined by ELISA. B16 murine melanoma cells were used as a positive control. C, A375/H-2D^b/gp100 and C918/H-2D^b/gp100 tumor-bearing mice (5 mice/group) were treated as described in Fig. 2A. Luciferase imaging showing *in vivo* trafficking of OFL-expressing pmel-1 T cells on day 5 after T-cell transfer. D, summary of quantitative imaging analysis of transferred T cells at the tumor sites, expressed as the average of photon flux within ROI. Data shown are expressed as mean + SEM and are representative of 2 independent experiments with similar results.

microenvironment that may explain the enhanced migration of adoptively transferred T cells. We thus harvested tumors from A375/H-2D^b/gp100 tumor-bearing mice treated with PLX4720 or vehicle alone, and made a tumor homogenate for protein array analysis. As shown in Fig. 4A, PLX4720 treatment significantly reduced the hVEGF production in tumors. Because chemokines are known to be essential for mediating T-cell trafficking, we also tested the intratumoral expression of a panel of 12 chemokines but found no significant differences between treatments. Inhibition of VEGF production was also confirmed by testing the supernatants from *in vitro* cell cultures of A375/H-2D^b/gp100 cells treated with PLX4720 (Supplementary Fig. S8).

VEGF is a key angiogenic factor known to stimulate endothelial cell growth, survival, migration, lumen formation, and vascular permeability (35). High levels of VEGF can induce vessel abnormalities that impair drug delivery and influx of immune cells into tumors, whereas vascular normalization by VEGF blockade or Rgs5 tumor cell deficiency can enhance the infiltration of adoptively transferred CD8⁺ T cells (35–37). Therefore, we next explored the possibility that reduced VEGF signaling in PLX4720-treated BRAF-mutant tumors was responsible for the enhanced infiltration by adoptively transferred T cells. As shown in Fig. 4B and C, *in vivo* blockade of the VEGF/VEGFR

interaction with anti-hVEGF Ab indeed enhanced pmel-1 T-cell infiltration into A375/H-2D^b/gp100 tumors. These results support the notion that administration of PLX4720 increases infiltration of adoptively transferred T cells via the inhibition of VEGF production by tumors.

PLX4720 treatment reduces the binding of c-myc to the VEGF promoter

Given that PLX4720 treatment is known to reduce ERK activation in tumor cells carrying a BRAF(V600E) mutation (9), we hypothesized that PLX4720 may repress VEGF transcription via inhibiting ERK-activated transcription factors involved in the direct regulation of VEGF transcription. To test this, we first confirmed that PLX4720 treatment inhibited the phosphorylation of ERK in A375/H-2D^b/gp100 tumor cells (Supplementary Fig. S9A). Examination of the proximal promoter region of human VEGF with TFSEARCH (<http://www.cbrc.jp/research/db/TFSEARCH.html>) identified potential consensus sites for multiple transcription factors, including c-myc, p300, and E2F1 (Supplementary Fig. S9B, and data not shown). Previous studies showed that c-myc and p300 were ERK-activated transcription factors, and E2F1 was a phosphoinositide 3-kinase (PI3K)-activated transcription factor (38–40). Using a ChIP assay, we have shown that c-myc is constitutively recruited to the VEGF promoter in A375/H-2D^b/gp100 cells

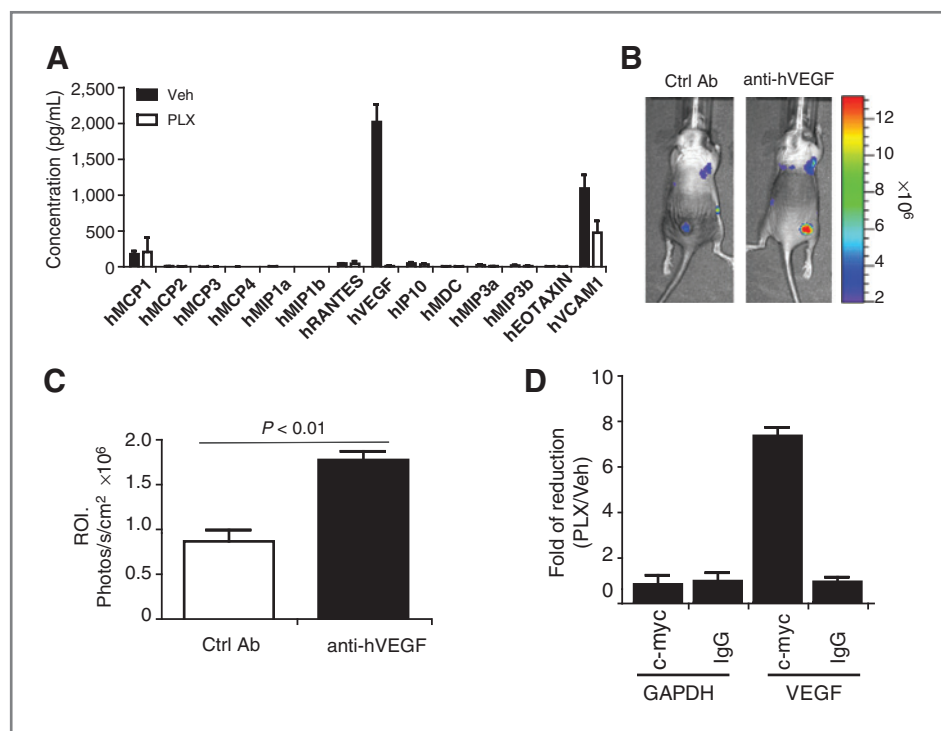


Figure 4. VEGF blockade *in vivo* increases tumor infiltration of adoptively transferred T cells. A, protein array analysis of cleared tumor lysates, conducted as described in Materials and Methods. B, B6 nude mice (5 mice/group) bearing A375/H-2D^b/gp100 tumors were treated with anti-hVEGF Ab or mouse IgG. Pictures showing intratumoral trafficking of OFL-expressing pmel-1 T cells represent results of imaging on day 5 after T-cell transfer. C, summary of the quantitative imaging analysis of transferred T cells at the tumor site on day 5 after T-cell transfer, expressed as the average photon flux within ROI. D, A375/H-2D^b/gp100 cells were treated with PLX4720 or DMSO for 2 hours, followed by ChIP assays using anti-c-myc antibody or control IgG. ChIP products were analyzed by RT-PCR using primers amplifying the promoter regions of human VEGF or the irrelevant gene *GAPDH*. Results were normalized to 1% total chromatin input, and presented as mean + SD of fold induction of PLX4720 versus Vehicle from 2 independent experiments.

(Fig. 4D). Furthermore, c-myc promoter binding, but not that of p300 or E2F1, was reduced approximately 5-fold following PLX4720 treatment (Supplementary Fig. S9C). These results strongly suggest that the spontaneous production of VEGF in A375/H-2D^b/gp100 cells is regulated by c-myc, and that PLX4720 reduces VEGF transcription via inhibition of c-myc binding to the VEGF promoter.

PLX4720-induced T-cell infiltration is abrogated in tumors overexpressing VEGF

To determine whether VEGF downregulation was indeed required for the enhanced intratumoral T-cell migration observed in PLX4720-treated mice, we next investigated whether this enhancement was impaired in tumors constitutively overexpressing VEGF. Thus, A375/H-2D^b/gp100 melanoma cells were transduced with hVEGF under the transcriptional control of the CMV promoter (Fig. 5A). VEGF-transduced melanoma cells maintained sensitivity to PLX4720 (Supplementary Fig. S10), but no longer showed a large decrease in VEGF secretion in response to PLX4720 treatment (Fig. 5B). We next analyzed B6 nude mice bearing either A375/H-2D^b/gp100 or A375/H-2D^b/gp100/VEGF tumors following treatment with ACT and PLX4720 by monitoring T-cell migration. As shown in Fig. 5C and D, augmented T-cell infiltration in response to PLX4720 treatment was abrogated in the A375/H-2D^b/gp100/VEGF tumors. These results support the notion that BRAF inhibition enhances T-cell migration to tumors through downregulation of VEGF production.

Intratumoral VEGF downregulation correlates with increased T-cell infiltration in melanoma patients treated with BRAF inhibitor

In light of our results in the mouse model, we next investigated whether VEGF was also downregulated in the tumors of patients with melanoma treated with BRAF inhibitor. Pretreatment or on-treatment tumor biopsies were harvested from 9 patients with melanoma, and immunohistochemical staining for VEGF was conducted. As shown in Fig. 6A and B, BRAF inhibitor treatment significantly downregulated VEGF expression in the majority (7/9) of patients, results which were confirmed by quantitative real-time PCR (qRT-PCR; Supplementary Fig. S11A and S11B). Examination of intratumoral T-cell infiltration was also conducted by staining the tumor samples for CD8 and reported separately by Dr. Jennifer Wargo's group. These results of patient samples are consistent with the data observed in the mouse model, and suggest that treatment of patients with BRAF inhibitor may also increase T-cell infiltration into tumors via inhibition of intratumoral VEGF production.

Discussion

To date, a number of specific kinase inhibitors that target BRAF(V600E) to treat melanoma have been generated and applied in clinical trials (8–10), with 50% to 70% of patients with BRAF(V600E) mutation showing objective clinical responses to treatment. However, despite these high

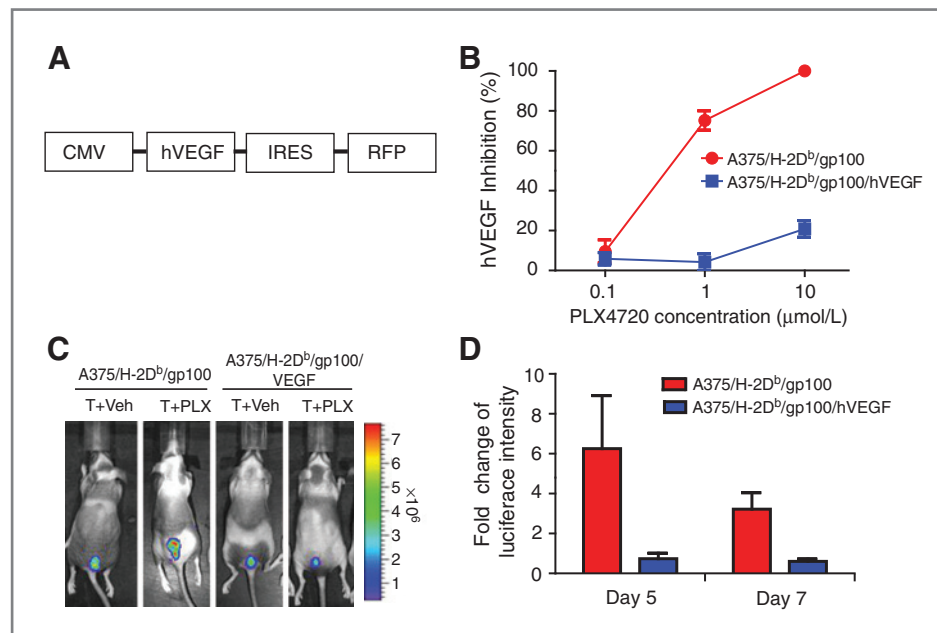


Figure 5. Overexpression of hVEGF abrogates increased infiltration of T cells into PLX4720-treated tumors. A, schematic representation of lentiviral vector expressing the *hVEGF* and *RFP* genes, separated by an IRES. A375/H-2D^b/gp100 melanoma cells were transduced, and VEGF-expressing cells were sorted on the basis of RFP expression. B, tumor cells with or without overexpression of hVEGF were incubated with PLX4720 for 24 hours, and VEGF concentrations in the supernatants were assessed by ELISA. C, B6 nude mice (5 mice/group) bearing A375/H-2D^b/gp100 tumors with or without overexpression of hVEGF were treated as described in Fig. 2A. Pictures show representative results of imaging on day 5 after T-cell transfer. D, graph depicting fold change in luciferase intensity, generated from quantitative imaging analysis of transferred T cells at the tumor site. Data shown are representative of 2 independent experiments with similar results.

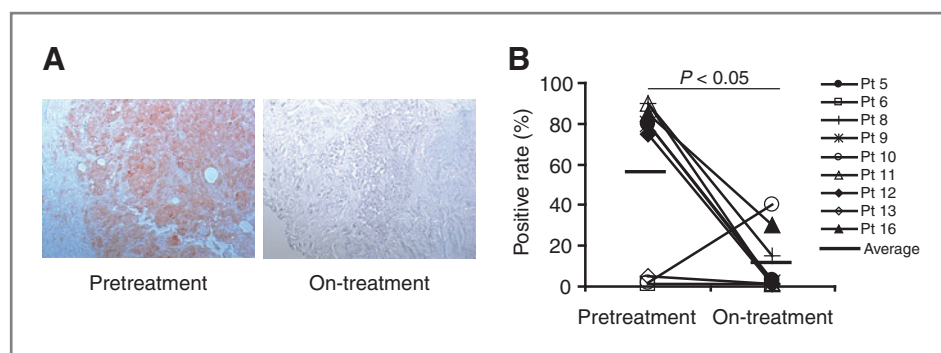


Figure 6. PLX4720 treatment downregulates tumoral VEGF in patients with melanoma. A, pre- and on-treatment VEGF expression in 2 representative tumor biopsies from BRAF inhibitor-treated patients, as determined by immunohistochemical analysis. Original magnification, $\times 200$. B, summary of quantitative analysis of VEGF expression in tumors from 9 BRAF inhibitor-treated patients. The percentage of VEGF-positive tumor cells in the tumor was evaluated by 2 pathologists in a blinded fashion.

initial response rates, responses are transient and recurrences with treatment-resistant disease typically occur within a year (12, 13, 41). Therefore, combinatorial approaches to treat melanoma are being actively explored.

ACT therapy using tumor-infiltrating lymphocytes is one of the most well-established immunotherapeutic approaches for cancer treatment (42). However, one of the important factors that limit the efficacy of this therapy is lack of migration of T cells into the tumor site (43, 44). Using a very sensitive bioluminescence imaging (BLI) system in murine models (27), we have previously shown that transduction of tumor-specific T cells with the CXCR2 chemokine receptor can improve the intratumoral migration of adoptively transferred T cells and enhance antitumor responses in murine models (28). In the current study, we tested whether the addition of a BRAF inhibitor could similarly enhance the antitumor activity of ACT *in vivo*. Using a xenograft human melanoma model, A375 transduced to express hgp100 and H-2D^b, we found that administration of PLX4720 could increase tumor infiltration of adoptively transferred gp100-specific T cells and improved antitumor responses. This effect was partially mediated by PLX4720-induced inhibition of VEGF production in melanoma cells. Analysis of tumor biopsies derived from BRAF inhibitor-treated patients with melanoma were consistent with the results found in the murine model, showing that BRAF inhibition could significantly downregulate tumoral VEGF expression, which correlated with increased tumor infiltration by T cells. Furthermore, our findings indicated that BRAF inhibition is capable of enhancing the antitumor activity of ACT therapy without impairing T-cell function.

VEGF, an immunosuppressive factor secreted by many tumors, can negatively impact the activity of tumor-infiltrating immune cells and stimulate the growth of tumor vasculature (45–47). RNA interference-mediated inhibition of BRAF(V600E) can decrease the production of VEGF in melanoma cells with mutant BRAF(V600E; ref. 21); however, it has remained unclear how constitutive activation of the BRAF-MAPK signaling pathway can influence VEGF production. Using a ChIP assay, we have shown that c-myc, but not p300 or E2F1, is constitutively recruited to

the VEGF promoter and that transcription and production of VEGF is reduced by PLX4720 in melanoma cells harboring the V600E mutation. Blocking of VEGF/VEGFR-2 interactions can upregulate endothelial adhesion molecules in tumor vessels, which can in turn increase the infiltration of leukocytes in tumors (48). Furthermore, administration of anti-VEGF Ab can significantly increase infiltration of adoptively transferred CD8⁺ T cells into tumor sites and improve antitumor responses (37). Using our xenogeneic mouse tumor model, we found that PLX4720 treatment significantly reduced the production of tumoral VEGF, and that the increased accumulation of tumor-infiltrating T cells was abrogated in melanoma overexpressing VEGF. Administration of anti-hVEGF Ab also increased tumor infiltration of pmel-1 T cells by 2- to 3-fold. Because PLX4720 treatment typically induced 5- to 10-fold higher levels of T-cell infiltration compared with vehicle treatment, it suggests that reduction of VEGF/VEGFR interactions is not the only mechanism responsible for the increased T-cell infiltration. Using gp100-negative tumor cells, PLX4720 treatment failed to increase T-cell trafficking to tumor sites. These findings suggest that tumor antigen expression also plays an important role in T-cell accumulation in tumors. These findings are consistent with our previous report that IFN- γ produced by tumor-antigen-activated T cells can induce CXCL10 expression in tumors, in turn resulting in more T-cell accumulation (49). Further studies will be required to identify additional mechanisms that may contribute to this combinational therapy regimen.

In this study, we have shown that administration of PLX4720 can clearly enhance the infiltration of transferred T cells and improve the antitumor responses induced by ACT. Our data are consistent with a recent clinical study showing that treatment of melanoma patients with a BRAF inhibitor leads to augmented T-cell infiltration into metastatic sites (11). Using a BRAF(V600E)-driven murine model, Koya and colleagues have recently shown that BRAF inhibition can increase MAPK signaling and intratumoral cytokines secretion by adoptively transferred T cells, leading to a beneficial antitumor effect (50). Collectively, the emerging evidence strongly suggests that combinations of

selective BRAF inhibitors with immunotherapy will result in enhanced benefits for patients with melanoma in the very near future.

Disclosure of Potential Conflicts of Interest

K.T. Flaherty is a consultant/advisory board member of Roche/Genentech, GlaxoSmithKline, and Novartis. M.A. Davies has a commercial research grant from GlaxoSmithKline, Genentech/Roche, and AstraZeneca, and is a consultant/advisory board member of GlaxoSmithKline, Genentech, and Novartis. No potential conflicts of interest were disclosed by the other authors.

Authors' Contributions

Conception and design: C. Liu, W. Peng, P. Hwu

Development of methodology: C. Liu, W. Peng, C. Xu, M. Zhang, H.S. Li, W.W. Overwijk, P. Hwu

Acquisition of data (provided animals, acquired and managed patients, provided facilities, etc.): C. Liu, W. Peng, C. Xu, J.A. Wargo, J.Q. Chen, H.S. Li, Y. Yang, D.T. Frederick, R.M. Mbofung, M. Whittington, K.T. Flaherty, L.G. Radvanyi, P. Hwu

Analysis and interpretation of data (e.g., statistical analysis, biostatistics, computational analysis): C. Liu, C. Xu, J.Q. Chen, H.S. Li, D.T. Frederick, K.T. Flaherty, S.E. Woodman, M.A. Davies, G. Lizée, P. Hwu

Writing, review, and/or revision of the manuscript: C. Liu, W. Peng, J.A. Wargo, D.T. Frederick, R.M. Mbofung, K.T. Flaherty, S.E. Woodman, M.A. Davies, L.G. Radvanyi, W.W. Overwijk, G. Lizée, P. Hwu

Administrative, technical, or material support (i.e., reporting or organizing data, constructing databases): C. Liu, C. Xu, Y. Lou, Y. Yang, Z.A. Cooper, W.W. Overwijk, P. Hwu

Study supervision: S.S. Watowich, P. Hwu

Grant Support

This work was supported in part by the following National Cancer Institute grants: R01 CA123182, R01 CA116206, and R01 CA143077. This research was also supported in part by Cancer Prevention Research Institute of Texas grant RP110248, Jurgen Sager & Transocean Melanoma Research Fund, El Paso Foundation for Melanoma Research, Miriam and Jim Mulva Melanoma Research Fund, the Gillson Logenbaugh Foundation, and Adelson Medical Research Foundation.

The costs of publication of this article were defrayed in part by the payment of page charges. This article must therefore be hereby marked *advertisement* in accordance with 18 U.S.C. Section 1734 solely to indicate this fact.

Received May 18, 2012; revised November 8, 2012; accepted November 13, 2012; published OnlineFirst November 30, 2012.

References

- Davies H, Bignell GR, Cox C, Stephens P, Edkins S, Clegg S, et al. Mutations of the BRAF gene in human cancer. *Nature* 2002;417:949–54.
- Wan PT, Garnett MJ, Roe SM, Lee S, Niculescu-Duvaz D, Good VM, et al. Mechanism of activation of the RAF-ERK signaling pathway by oncogenic mutations of B-RAF. *Cell* 2004;116:855–67.
- Fedorenko IV, Paraiso KH, Smalley KS. Acquired and intrinsic BRAF inhibitor resistance in BRAF V600E mutant melanoma. *Biochem Pharmacol* 2011;82:201–9.
- Davies MA, Samuels Y. Analysis of the genome to personalize therapy for melanoma. *Oncogene* 2010;29:5545–55.
- Gray-Schopfer V, Wellbrock C, Marais R. Melanoma biology and new targeted therapy. *Nature* 2007;445:851–7.
- Tiacci E, Trifonov V, Schiavoni G, Holmes A, Kern W, Martelli MP, et al. BRAF mutations in hairy-cell leukemia. *N Engl J Med* 2011;364:2305–15.
- Jakob JA, Bassett RL Jr, Ng CS, Curry JL, Joseph RW, Alvarado GC, et al. NRAS mutation status is an independent prognostic factor in metastatic melanoma. *Cancer* 2012;118:4014–23.
- Bollag G, Hirth P, Tsai J, Zhang J, Ibrahim PN, Cho H, et al. Clinical efficacy of a RAF inhibitor needs broad target blockade in BRAF-mutant melanoma. *Nature* 2010;467:596–9.
- Tsai J, Lee JT, Wang W, Zhang J, Cho H, Mamo S, et al. Discovery of a selective inhibitor of oncogenic B-Raf kinase with potent antimelanoma activity. *Proc Natl Acad Sci U S A* 2008;105:3041–6.
- Kefford R, Arkenau H, Brown MP, Millward M, Infante JR, Long GV, et al. Phase I/II study of GSK2118436, a selective inhibitor of oncogenic mutant BRAF kinase, in patients with metastatic melanoma and other solid tumors. *J Clin Oncol* 28:15s, 2010 (suppl; abstr 8503).
- Wilmott JS, Long GV, Howle JR, Haydu LE, Sharma RN, Thompson JF, et al. Selective BRAF inhibitors induce marked T-cell infiltration into human metastatic melanoma. *Clin Cancer Res* 2012;18:1386–94.
- Flaherty KT, Puzanov I, Kim KB, Ribas A, McArthur GA, Sosman JA, et al. Inhibition of mutated, activated BRAF in metastatic melanoma. *N Engl J Med* 2010;363:809–19.
- Hersey P, Smalley KS, Weeraratna A, Bosenberg M, Zhang XD, Haass NK, et al. Meeting report from the 7th International Melanoma Congress, Sydney, November, 2010. *Pigment Cell Melanoma Res* 2011;24:e1–15.
- Nazarian R, Shi H, Wang Q, Kong X, Koya RC, Lee H, et al. Melanomas acquire resistance to B-RAF(V600E) inhibition by RTK or N-RAS upregulation. *Nature* 2010;468:973–7.
- Wagle N, Emery C, Berger MF, Davis MJ, Sawyer A, Pochanard P, et al. Dissecting therapeutic resistance to RAF inhibition in melanoma by tumor genomic profiling. *J Clin Oncol* 2011;29:3085–96.
- Villanueva J, Vultur A, Lee JT, Somasundaram R, Fukunaga-Kalabis M, Cipolla AK, et al. Acquired resistance to BRAF inhibitors mediated by a RAF kinase switch in melanoma can be overcome by cotargeting MEK and IGF-1R/PI3K. *Cancer Cell* 2010;18:683–95.
- Paraiso KH, Fedorenko IV, Cantini LP, Munko AC, Hall M, Sondak VK, et al. Recovery of phospho-ERK activity allows melanoma cells to escape from BRAF inhibitor therapy. *Br J Cancer* 2010;102:1724–30.
- Johannessen CM, Boehm JS, Kim SY, Thomas SR, Wardwell L, Johnson LA, et al. COT drives resistance to RAF inhibition through MAP kinase pathway reactivation. *Nature* 2010;468:968–72.
- Jiang CC, Lai F, Thorne RF, Yang F, Liu H, Hersey P, et al. MEK-independent survival of B-RAFV600E melanoma cells selected for resistance to apoptosis induced by the RAF inhibitor PLX4720. *Clin Cancer Res* 2011;17:721–30.
- Smalley KS, Flaherty KT. Integrating BRAF/MEK inhibitors into combination therapy for melanoma. *Br J Cancer* 2009;100:431–5.
- Sumimoto H, Imabayashi F, Iwata T, Kawakami Y. The BRAF-MAPK signaling pathway is essential for cancer-immune evasion in human melanoma cells. *J Exp Med* 2006;203:1651–6.
- Kono M, Dunn IS, Durda PJ, Butera D, Rose LB, Haggerty TJ, et al. Role of the mitogen-activated protein kinase signaling pathway in the regulation of human melanocytic antigen expression. *Mol Cancer Res* 2006;4:779–92.
- Boni A, Cogdill AP, Dang P, Udayakumar D, Njauw CN, Sloss CM, et al. Selective BRAFV600E inhibition enhances T-cell recognition of melanoma without affecting lymphocyte function. *Cancer Res* 2010;70:5213–9.
- Jiang X, Zhou J, Giobbie-Hurder A, Wargo JA, Hodi FS. The paradoxical activation of MAPK in melanoma cells resistant to BRAF inhibition promotes PD-L1 expression that is reversible by MEK and PI3K inhibition. *Clin Cancer Res*. 2012 Oct 24. [Epub ahead of print].
- Hong DS, Vence LM, Falchook GS, Radvanyi LG, Liu C, Goodman VL, et al. Braf(V600) inhibitor Gsk2118436 targeted inhibition of mutant Braf in cancer patients does not impair overall immune competency. *Clin Cancer Res* 2012;18:2326–35.
- Johnson LA, Heemskerk B, Powell DJ Jr, Cohen CJ, Morgan RA, Dudley ME, et al. Gene transfer of tumor-reactive TCR confers both high avidity and tumor reactivity to nonreactive peripheral blood mononuclear cells and tumor-infiltrating lymphocytes. *J Immunol* 2006;177:6548–59.
- Rabinovich BA, Ye Y, Etto T, Chen JQ, Levitsky HI, Overwijk WW, et al. Visualizing fewer than 10 mouse T cells with an enhanced firefly luciferase in immunocompetent mouse models of cancer. *Proc Natl Acad Sci U S A* 2008;105:14342–6.

28. Peng W, Ye Y, Rabinovich BA, Liu C, Lou Y, Zhang M, et al. Transduction of tumor-specific T cells with CXCR2 chemokine receptor improves migration to tumor and antitumor immune responses. *Clin Cancer Res* 2010;16:5458–68.
29. Steinman RM, Inaba K, Turley S, Pierre P, Mellman I. Antigen capture, processing, and presentation by dendritic cells: recent cell biological studies. *Hum Immunol* 1999;60:562–7.
30. Lou Y, Wang G, Lizee G, Kim GJ, Finkelstein SE, Feng C, et al. Dendritic cells strongly boost the antitumor activity of adoptively transferred T cells *in vivo*. *Cancer Res* 2004;64:6783–90.
31. Overwijk WW, Theoret MR, Finkelstein SE, Surman DR, de Jong LA, Vyth-Dreese FA, et al. Tumor regression and autoimmunity after reversal of a functionally tolerant state of self-reactive CD8⁺ T cells. *J Exp Med* 2003;198:569–80.
32. Poulidakos PI, Zhang C, Bollag G, Shokat KM, Rosen N. RAF inhibitors transactivate RAF dimers and ERK signalling in cells with wild-type BRAF. *Nature* 2010;464:427–30.
33. Halaban R, Zhang W, Bacchiocchi A, Cheng E, Parisi F, Ariyan S, et al. PLX4032, a selective BRAF(V600E) kinase inhibitor, activates the ERK pathway and enhances cell migration and proliferation of BRAF melanoma cells. *Pigment Cell Melanoma Res* 2010;23:190–200.
34. Hatzivassiliou G, Song K, Yen I, Brandhuber BJ, Anderson DJ, Alvarado R, et al. RAF inhibitors prime wild-type RAF to activate the MAPK pathway and enhance growth. *Nature* 2010;464:431–5.
35. Carmeliet P, Jain RK. Principles and mechanisms of vessel normalization for cancer and other angiogenic diseases. *Nat Rev Drug Discov* 2011;10:417–27.
36. Hamzah J, Jugold M, Kiessling F, Rigby P, Manzur M, Marti HH, et al. Vascular normalization in Rgs5-deficient tumours promotes immune destruction. *Nature* 2008;453:410–4.
37. Shrimali RK, Yu Z, Theoret MR, Chinnasamy D, Restifo NP, Rosenberg SA. Antiangiogenic agents can increase lymphocyte infiltration into tumor and enhance the effectiveness of adoptive immunotherapy of cancer. *Cancer Res* 2010;70:6171–80.
38. Marampon F, Bossi G, Ciccarelli C, Di Rocco A, Sacchi A, Pestell RG, et al. MEK/ERK inhibitor U0126 affects *in vitro* and *in vivo* growth of embryonal rhabdomyosarcoma. *Mol Cancer Ther* 2009;8:543–51.
39. Jun JH, Yoon WJ, Seo SB, Woo KM, Kim GS, Ryoo HM, et al. BMP2-activated Erk/MAP kinase stabilizes Runx2 by increasing p300 levels and histone acetyltransferase activity. *J Biol Chem* 2010;285:36410–9.
40. Lee KY, Lee JW, Nam HJ, Shim JH, Song Y, Kang KW. PI3-kinase/p38 kinase-dependent E2F1 activation is critical for Pin1 induction in tamoxifen-resistant breast cancer cells. *Mol Cells* 2011;32:107–11.
41. Sosman JA, Kim KB, Schuchter L, Gonzalez R, Pavlick AC, Weber JS, et al. Survival in BRAF V600-mutant advanced melanoma treated with vemurafenib. *N Engl J Med* 2012;366:707–14.
42. Rosenberg SA, Dudley ME. Adoptive cell therapy for the treatment of patients with metastatic melanoma. *Curr Opin Immunol* 2009;21:233–40.
43. Blattman JN, Greenberg PD. Cancer immunotherapy: a treatment for the masses. *Science* 2004;305:200–5.
44. Pockaj BA, Sherry RM, Wei JP, Yannelli JR, Carter CS, Leitman SF, et al. Localization of 111indium-labeled tumor infiltrating lymphocytes to tumor in patients receiving adoptive immunotherapy. Augmentation with cyclophosphamide and correlation with response. *Cancer* 1994;73:1731–7.
45. Ohm JE, Carbone DP. VEGF as a mediator of tumor-associated immunodeficiency. *Immunol Res* 2001;23:263–72.
46. Mulligan JK, Day TA, Gillespie MB, Rosenzweig SA, Young MR. Secretion of vascular endothelial growth factor by oral squamous cell carcinoma cells skews endothelial cells to suppress T-cell functions. *Hum Immunol* 2009;70:375–82.
47. Folkman J. Angiogenesis. *Annu Rev Med* 2006;57:1–18.
48. Dirx AE, oude Egbrink MG, Castermans K, van der Schaft DW, Thijssen VL, Dings RP, et al. Anti-angiogenesis therapy can overcome endothelial cell anergy and promote leukocyte-endothelium interactions and infiltration in tumors. *FASEB J* 2006;20:621–30.
49. Peng W, Liu C, Xu C, Lou Y, Chen J, Yang Y, et al. PD-1 blockade enhances T-cell migration to tumors by elevating IFN-gamma inducible chemokines. *Cancer Res* 2012;72:5209–18.
50. Koya RC, Mok S, Otte N, Blacketer KJ, Comin-Anduix B, Tumei PC, et al. BRAF Inhibitor Vemurafenib Improves the Antitumor Activity of Adoptive Cell Immunotherapy. *Cancer Res* 2012;72:3928–37.

Clinical Cancer Research

BRAF Inhibition Increases Tumor Infiltration by T cells and Enhances the Antitumor Activity of Adoptive Immunotherapy in Mice

Chengwen Liu, Weiyi Peng, Chunyu Xu, et al.

Clin Cancer Res 2013;19:393-403. Published OnlineFirst November 30, 2012.

Updated version Access the most recent version of this article at:
doi:[10.1158/1078-0432.CCR-12-1626](https://doi.org/10.1158/1078-0432.CCR-12-1626)

Supplementary Material Access the most recent supplemental material at:
<http://clincancerres.aacrjournals.org/content/suppl/2012/11/30/1078-0432.CCR-12-1626.DC1>

Cited articles This article cites 49 articles, 19 of which you can access for free at:
<http://clincancerres.aacrjournals.org/content/19/2/393.full#ref-list-1>

Citing articles This article has been cited by 41 HighWire-hosted articles. Access the articles at:
<http://clincancerres.aacrjournals.org/content/19/2/393.full#related-urls>

E-mail alerts [Sign up to receive free email-alerts](#) related to this article or journal.

Reprints and Subscriptions To order reprints of this article or to subscribe to the journal, contact the AACR Publications Department at pubs@aacr.org.

Permissions To request permission to re-use all or part of this article, use this link
<http://clincancerres.aacrjournals.org/content/19/2/393>.
Click on "Request Permissions" which will take you to the Copyright Clearance Center's (CCC) Rightslink site.